Morphology studies and resolved spectroscopy of the Vela Jr. Supernova remnant with H.E.S.S.

Iurii Sushch, Manuel Paz Arribas, Nukri Komin, Ullrich Schwanke for the H.E.S.S. Collaboration

DESY, Zeuthen, Germany

North-West University, Potchefstroom, South Africa

H.E.S.S.

DESY

Vela Jr. SNR

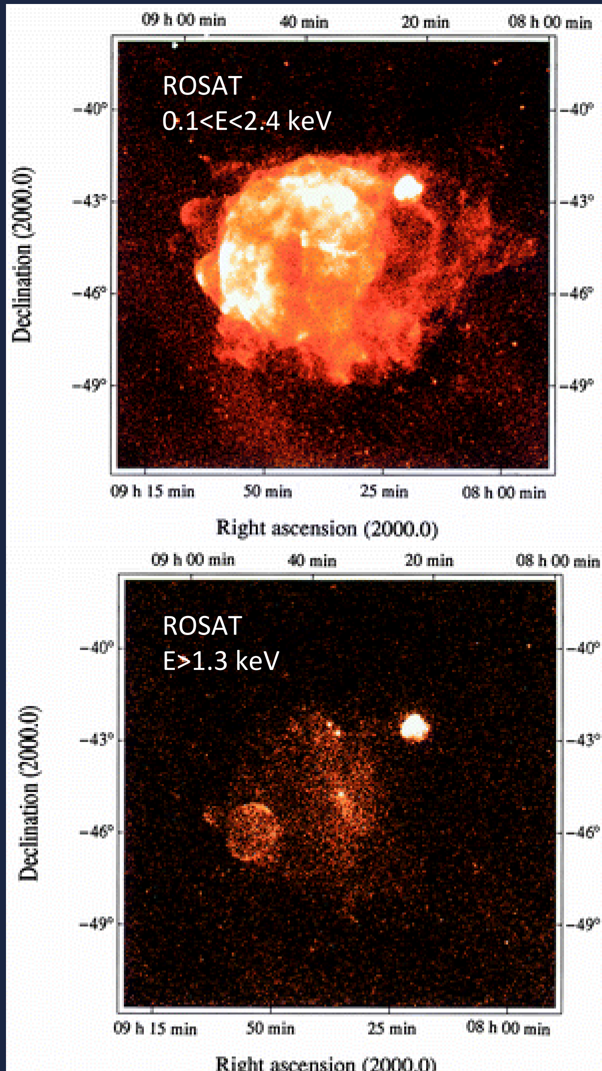

Aschenbach 1998, Nature, 396, 141

- Young shell-type SNR
- Broadband non-thermal emission from radio to very-high-energy gamma-rays (E>100 GeV)
- Resolved shell at TeV energies

- Age: 1700 – 4300 yr
- Distance: 500 – 1000 pc. 750 pc (Katsuda et al. 2008) is used
- Probably core-collapse

TeV emission

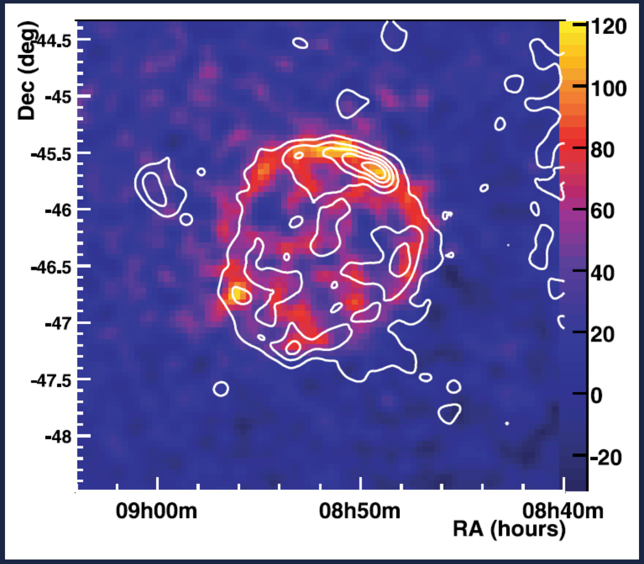

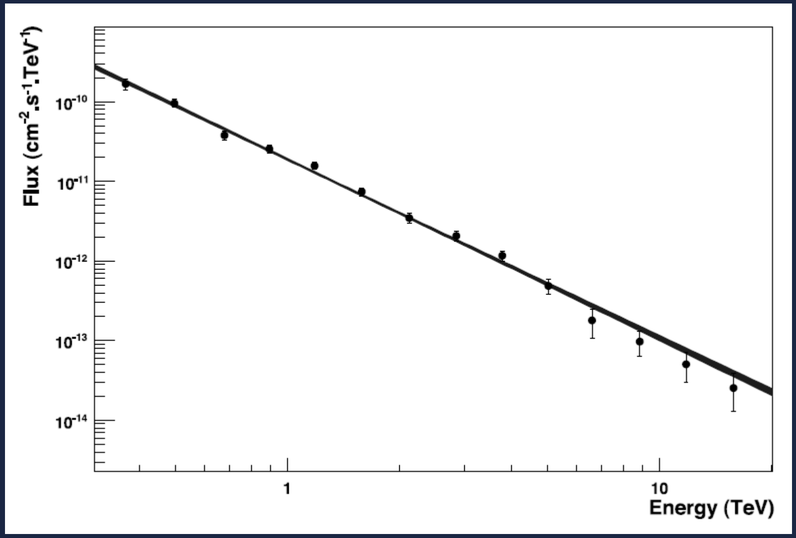

Aharonian et al. 2007

- The first TeV detection was by CANGAROO (Muraishi et al. 2000)
- And then H.E.S.S. (Aharonian et al. 2004, 2007)
- Clear shell-like morphology with a thin shell
- Good correlation with the X-ray emission
- No evidence of cut-off in the energy spectrum

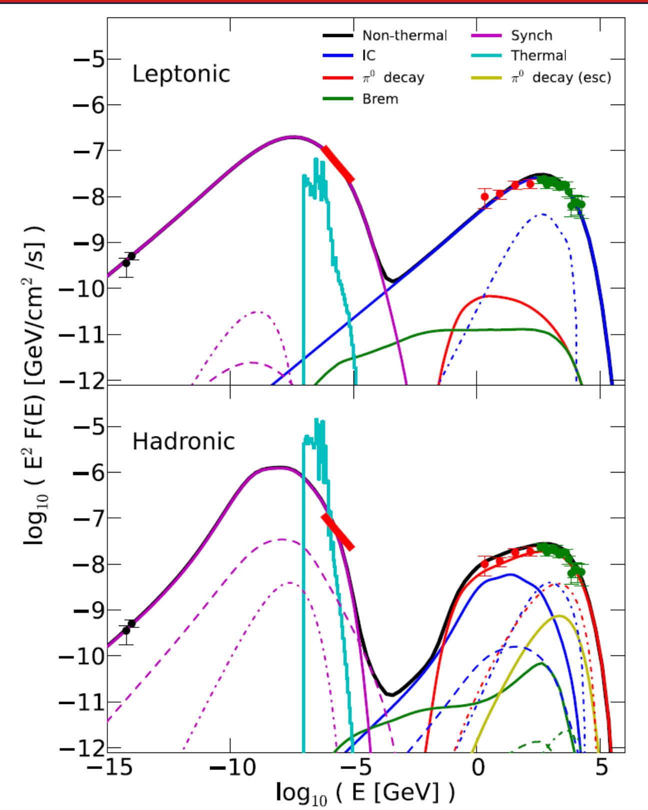

Lee et al. 2013

see Lee’s talk

Origin: leptonic or hadronic?

- Leptonic models suggest low magnetic field (~ 5 μG), But sharp X-ray filaments suggest strong magnetic field amplification (100-500 μG) in case of fast synchrotron cooling (Bamba et al. 2005, Berezhko et al. 2009)
- Hadronic models require high density of the ambient medium which contradicts the non-detection of the X-ray thermal emission. May be interaction with the clumpy environment with dense small clouds.
- Steepening of the X-ray spectrum towards the observer explained by synchrotron cooling with ~ 10 μG magnetic field, but high (~ 100 TeV) electron cut-off energy

see Fukui’s talk

Kishishita et al. 2013

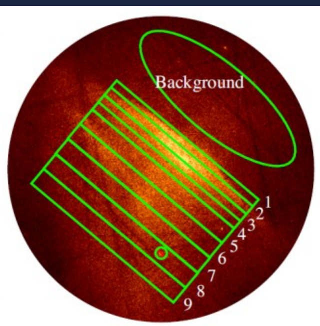

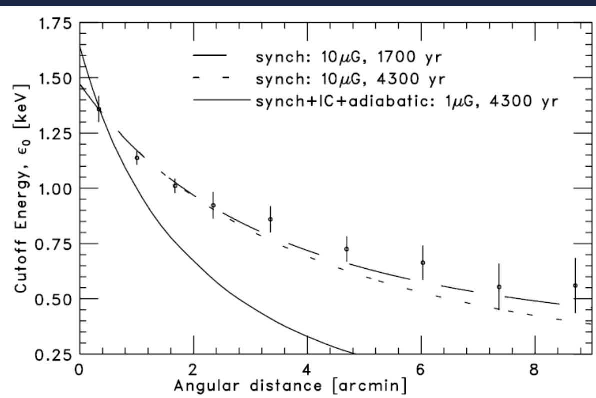

New data

- Data used in this analysis were taken between 2004 and 2009
- Data taken with the initial phase of H.E.S.S. (4 telescopes)
- The analysis of data up to the end of 2005 has already been published in *Aharonian et al. 2005 & 2007*
- Rough doubling of the data set
- Enables detailed morphological and spectral studies, including spatially-resolved spectroscopy

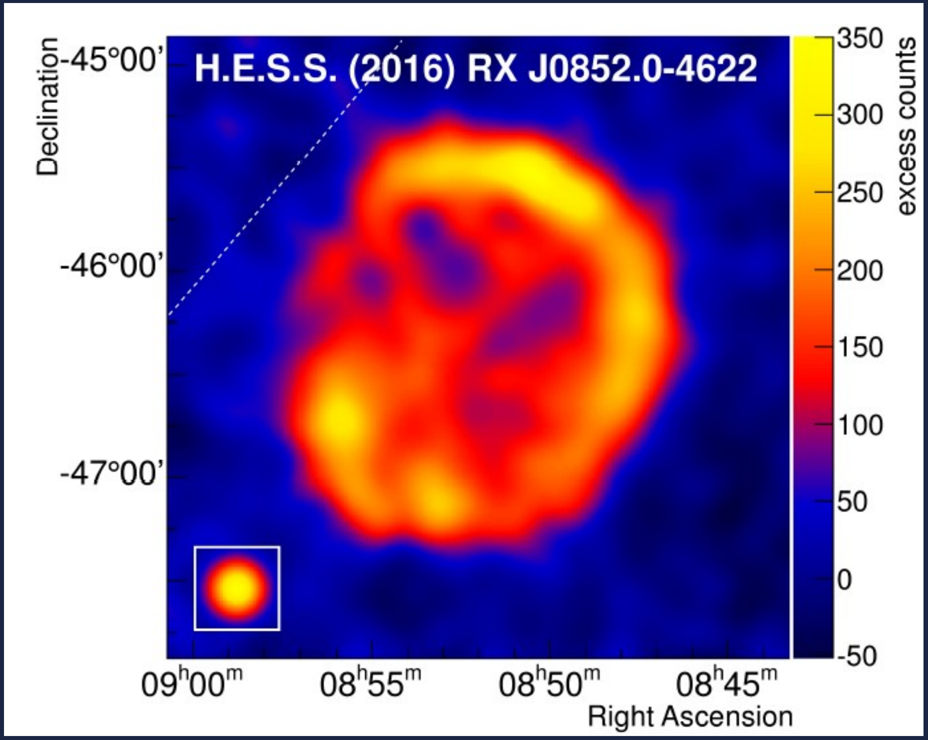

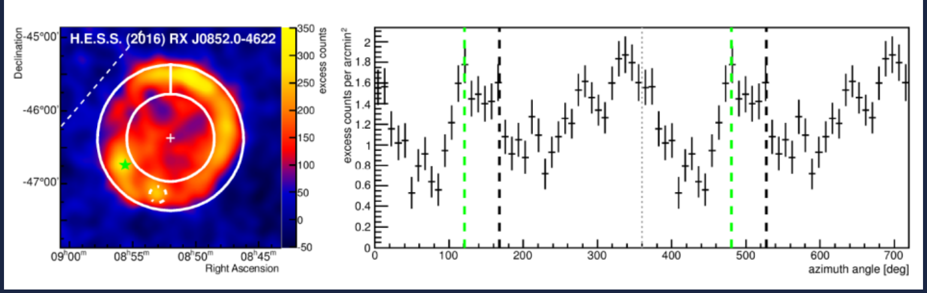

Morphology

- Well resolved shell-like morphology
- North-western rim is brighter than the south-eastern part of the shell
- Enhanced emission in the south-east is coincident with a pulsar PSR J0855-4644 and probably coming from a TeV PWN
- Another local hot spot in the south

Spectrum

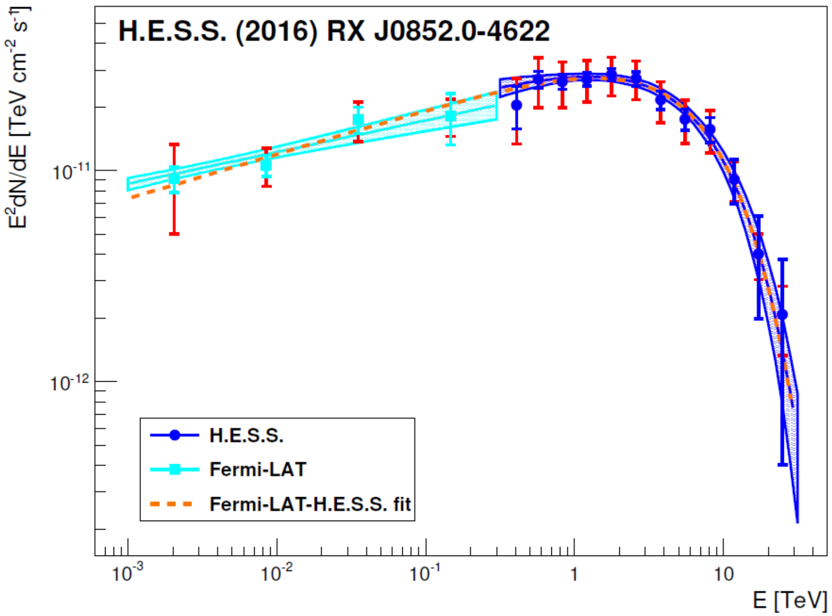

- Higher flux than found in previous studies. Lower flux found in previous studies was due to the lack of correction for the degradation of the telescopes' reflectivity
- Updated flux estimate makes Vela Jr the brightest steady source above 1 TeV
- Clear curvature in the spectrum best fit with the exponential cut-off
- Good connection with the GeV spectrum measured by Fermi-LAT

parameter		H.E.S.S.	H.E.S.S. and *Fermi*-LAT
Φ_0	$[10^{-12}\ \mathrm{cm^{-2}s^{-1}TeV^{-1}}]$	$32.2 \pm 1.5_{stat} \pm 7.1_{syst}$	$31.6 \pm 1.4_{stat} \pm 7.6_{syst}$
Γ		$1.81 \pm 0.08_{stat} \pm 0.20_{syst}$	$1.79 \pm 0.02_{stat} \pm 0.10_{syst}$
E_{cut}	[TeV]	$6.7 \pm 1.2_{stat} \pm 1.2_{syst}$	$6.6 \pm 0.7_{stat} \pm 1.3_{syst}$
E_0	[TeV]	1	1
$E_{min} - E_{max}$	[TeV]	0.3 – 30	0.001 – 30
$F(> 1\ \mathrm{TeV})$	$[10^{-12}\ \mathrm{cm^{-2}s^{-1}}]$	$23.4 \pm 0.7_{stat} \pm 4.9_{syst}$	
$F(0.3 - 30\ \mathrm{TeV})$	$[10^{-12}\ \mathrm{cm^{-2}s^{-1}}]$	$84.1 \pm 4.3_{stat} \pm 21.7_{syst}$	

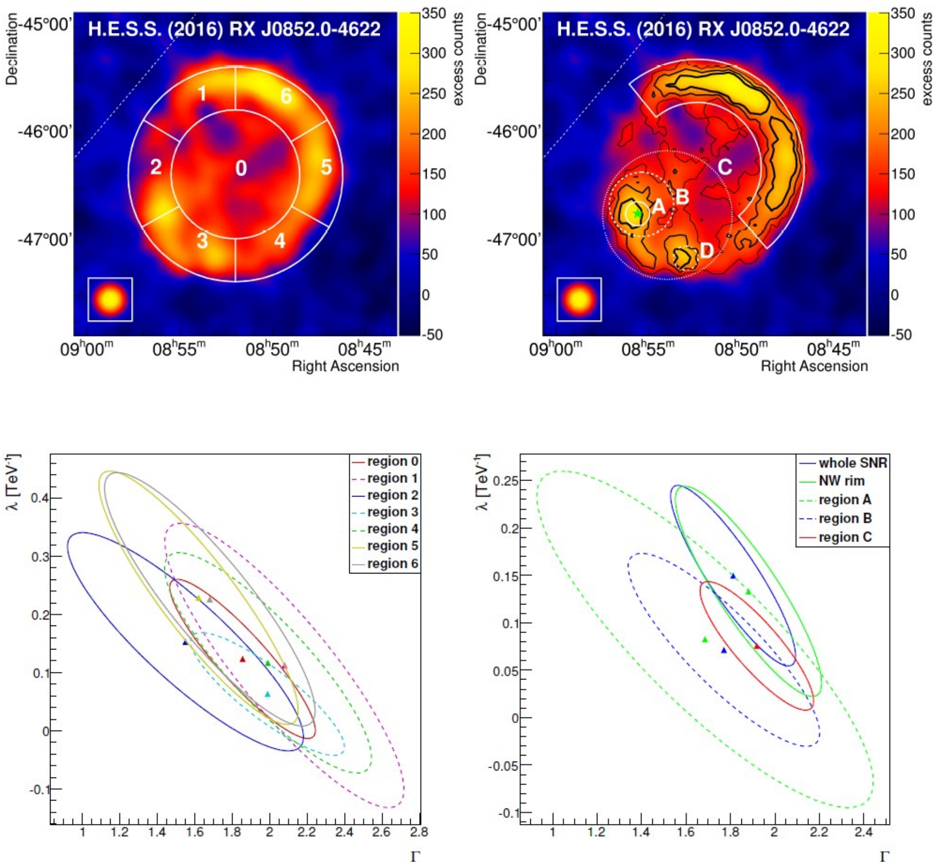

Spatially resolved spectroscopy

- Region 0 and regions in the NW rim show the preference for a cut-off in the spectrum

Spatially resolved spectroscopy

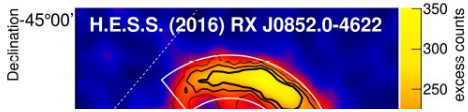

region	Φ_0 $[10^{-12}\,\mathrm{cm}^{-2}\mathrm{s}^{-1}\mathrm{TeV}^{-1}]$	Γ	E_{cut} [TeV]	$F(>1\,\mathrm{TeV})$ $[10^{-12}\,\mathrm{cm}^{-2}\mathrm{s}^{-1}]$	$F(0.3-30\,\mathrm{TeV})$ $[10^{-12}\,\mathrm{cm}^{-2}\mathrm{s}^{-1}]$	sign
whole SNR	$32.2 \pm 1.5(\pm 7.1)$	$1.81 \pm 0.08(\pm 0.20)$	$6.7 \pm 1.2(\pm 1.2)$	$23.4 \pm 0.7(\pm 4.9)$	$84.1 \pm 4.3(\pm 21.7)$	7.7σ
NW rim	$12.4 \pm 0.7(\pm 3.1)$	$1.88 \pm 0.10(\pm 0.20)$	$7.5 \pm 1.8(\pm 1.5)$	$8.9 \pm 0.4(\pm 2.2)$	$33.7 \pm 2.0(\pm 8.4)$	5.6σ
0	$8.9 \pm 0.6(\pm 2.2)$	$1.85 \pm 0.11(\pm 0.20)$	$8.1 \pm 2.6(\pm 1.6)$	$6.7 \pm 0.3(\pm 1.7)$	$24.1 \pm 1.6(\pm 6.0)$	4.5σ
1	$3.5 \pm 0.4(\pm 0.9)$	$2.08 \pm 0.19(\pm 0.20)$	$8.9 \pm 5.6(\pm 1.8)$	$2.34 \pm 0.20(\pm 0.59)$	$10.5 \pm 1.1(\pm 2.6)$	2.1σ
2	$2.4 \pm 0.3(\pm 0.6)$	$1.55 \pm 0.18(\pm 0.20)$	$6.5 \pm 2.3(\pm 1.3)$	$2.12 \pm 0.16(\pm 0.53)$	$5.9 \pm 0.7(\pm 1.5)$	3.9σ
3	$4.0 \pm 0.3(\pm 1.0)$	$1.99 \pm 0.12(\pm 0.20)$	$15.8 \pm 7.7(\pm 3.2)$	$3.19 \pm 0.19(\pm 0.80)$	$12.1 \pm 1.0(\pm 3.0)$	2.3σ
4	$3.8 \pm 0.4(\pm 1.0)$	$1.99 \pm 0.16(\pm 0.20)$	$8.6 \pm 4.0(\pm 1.7)$	$2.64 \pm 0.20(\pm 0.66)$	$10.9 \pm 1.1(\pm 2.7)$	2.7σ
5	$4.4 \pm 0.4(\pm 1.1)$	$1.62 \pm 0.15(\pm 0.20)$	$4.4 \pm 1.2(\pm 0.9)$	$2.99 \pm 0.17(\pm 0.75)$	$9.9 \pm 0.8(\pm 2.5)$	5.5σ
6	$5.2 \pm 0.5(\pm 1.3)$	$1.68 \pm 0.16(\pm 0.20)$	$4.4 \pm 1.2(\pm 0.9)$	$3.43 \pm 0.22(\pm 0.86)$	$12.0 \pm 1.1(\pm 3.0)$	4.9σ
A	$0.64 \pm 0.10(\pm 0.16)$	$1.69 \pm 0.22(\pm 0.20)$	$12.1 \pm 7.6(\pm 2.4)$	$0.62 \pm 0.07(\pm 0.15)$	$1.8 \pm 0.3(\pm 0.4)$	1.8σ
B	$2.34 \pm 0.19(\pm 0.59)$	$1.77 \pm 0.13(\pm 0.20)$	$14.0 \pm 5.8(\pm 2.8)$	$2.18 \pm 0.14(\pm 0.55)$	$6.6 \pm 0.7(\pm 1.7)$	2.7σ
C	$10.0 \pm 0.5(\pm 2.5)$	$1.92 \pm 0.07(\pm 0.20)$	$13.2 \pm 3.4(\pm 2.6)$	$8.2 \pm 0.3(\pm 2.1)$	$29.5 \pm 1.6(\pm 7.4)$	4.5σ
D	$0.81 \pm 0.12(\pm 0.20)$	$2.02 \pm 0.25(\pm 0.20)$	$11.2 \pm 9.3(\pm 2.2)$	$0.59 \pm 0.07(\pm 0.15)$	$2.4 \pm 0.4(\pm 0.6)$	1.4σ
B′	$1.88 \pm 0.18(\pm 0.47)$	$1.78 \pm 0.15(\pm 0.20)$	$13.9 \pm 6.9(\pm 2.8)$	$1.73 \pm 0.13(\pm 0.43)$	$5.4 \pm 0.6(\pm 1.3)$	2.3σ
C′	$6.7 \pm 0.4(\pm 1.7)$	$1.91 \pm 0.09(\pm 0.20)$	$12.2 \pm 3.8(\pm 2.4)$	$5.4 \pm 0.3(\pm 1.4)$	$19.6 \pm 1.4(\pm 4.9)$	3.8σ

Spatially resolved spectroscopy

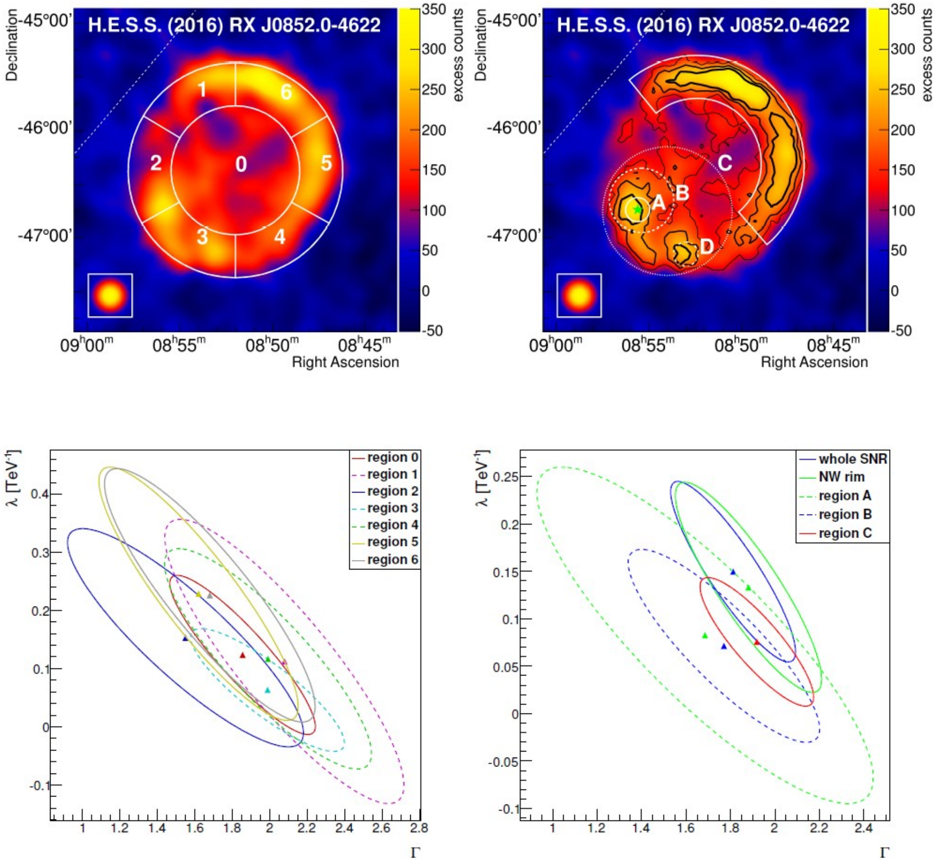

- Region 0 and regions in the NW rim show the preference for a cut-off in the spectrum
- No significant variation in the spectral properties
- Region B shows some evidence for harder spectrum (probably because of the PWN), but still not very significant (3.5σ pre-trials and 2.6σ post-trials)
- Region D doesn't show any deviation from the rest of remnant suggesting that this southern hot spot is associated with the SNR

Present-time parent particle population

- Lack of spectral variation suggests that parent particle distribution is essentially the same across the remnant
- Smooth connection with the GeV measurement and well-resolved cut-off allows us to directly extract the present-time parent particle population by fitting the GeV – TeV spectrum
- The spectrum of the parent particle population is assumed to follow the power law with an exponential cut-off in both leptonic and hadronic scenarios

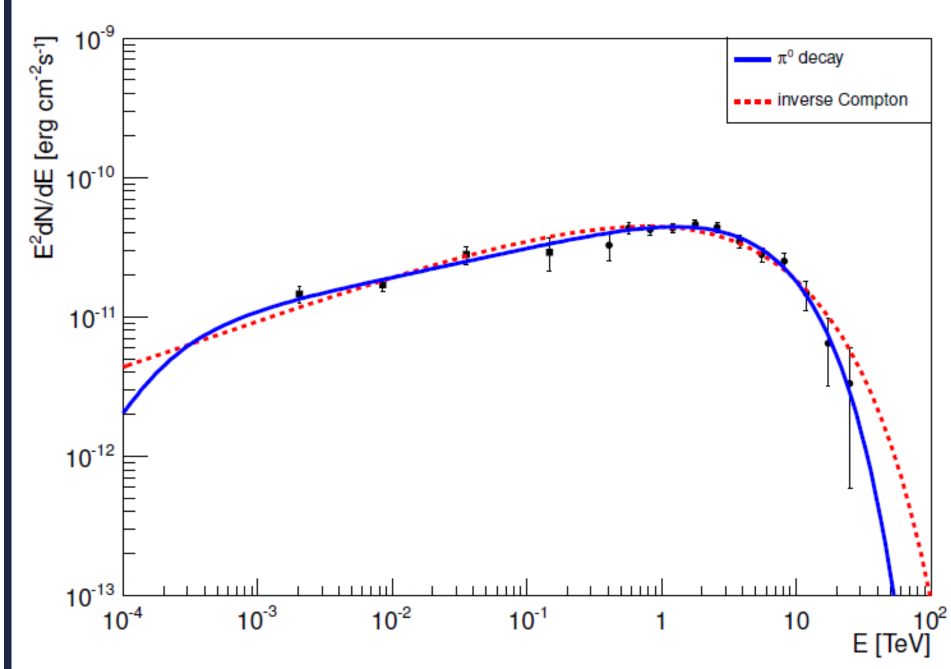

scenario	parameter		value
hadronic	$\frac{N_{0,p}}{4\pi d^2}\,[n]^{-1}$	$[10^4\ \mathrm{TeV}^{-1}\mathrm{cm}^{-2}]$	$7.8 \pm 0.3(\pm 2.0)$
	p_p		$1.83 \pm 0.02(\pm 0.11)$
	$E_{\mathrm{cut,p}}$	[TeV]	$55 \pm 6(\pm 13)$
	$W_p\,[n]^{-1}$	$[10^{49}\mathrm{erg}]$	$7.1 \pm 0.3(\pm 1.9)$
leptonic	$\frac{N_{0,e}}{4\pi d^2}$	$[10^2\ \mathrm{TeV}^{-1}\mathrm{cm}^{-2}]$	$7.8 \pm 0.6(\pm 3.1)$
	p_e		$2.33 \pm 0.03(\pm 0.33)$
	$E_{\mathrm{cut,e}}$	[TeV]	$27 \pm 1(\pm 12)$
	W_e	$[10^{47}\mathrm{erg}]$	$4.1 \pm 0.3(\pm 1.7)$

Leptonic scenario

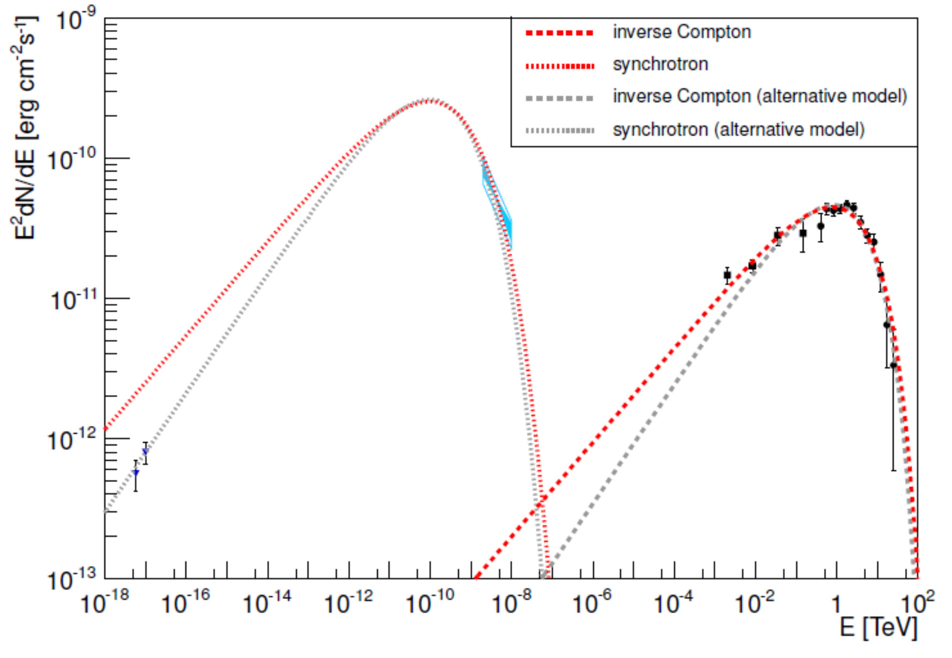

Kishishita et al. 2013

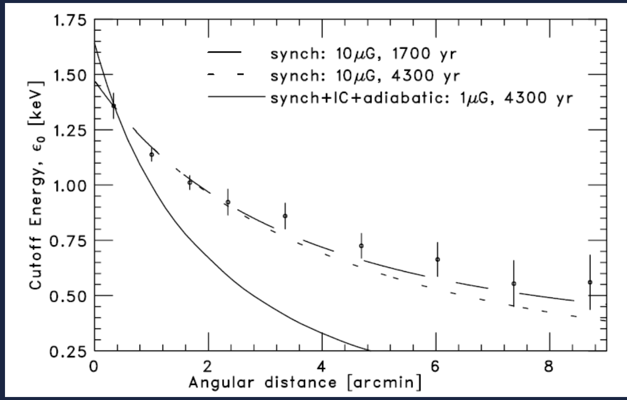

- For the derived parameters of the parent electron population, observed X-ray emission suggests a low magnetic field of 7 μG (average across the remnant)
- Radio data can also be accommodated within the uncertainties (the grey line is constructed by changing spectral parameters by 0.6σ)
- Synchrotron cooling effects are negligible
- The electron spectrum may be limited by the age of the SNR
- Still in conflict with filaments in the NW rim (if they are limited by synchrotron cooling)

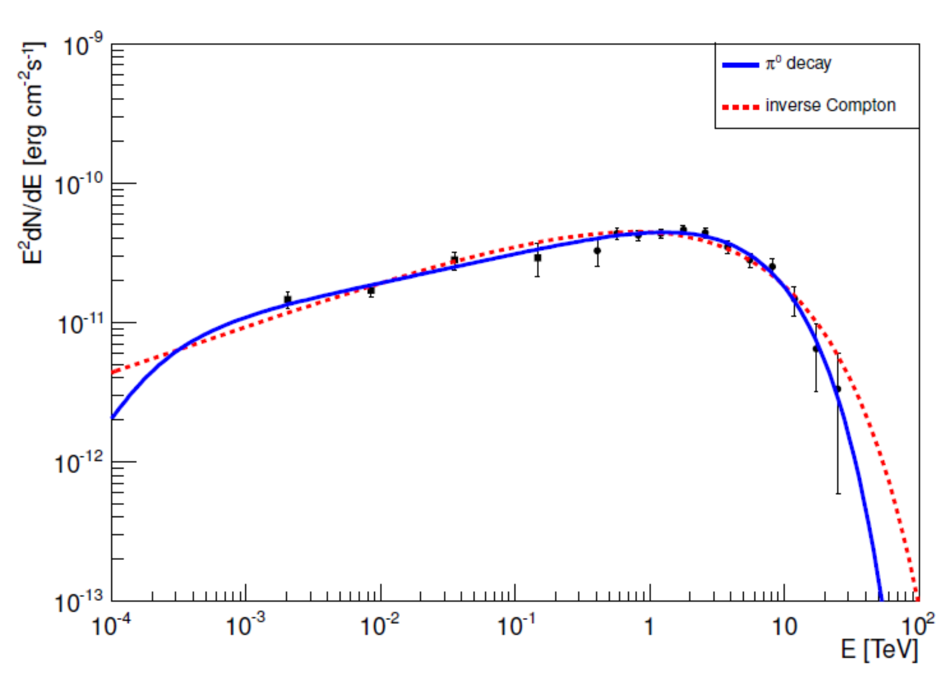

Hadronic scenario

- Requires ~ 1 cm^{-3} density of the ambient medium
- Lack of X-ray thermal emission suggest the density ~ 2 magnitudes lower than that.
- Can be solved for the SNR expanding in a very inhomogeneous clumpy environment
- Indeed, the SNR seems to be surrounded by clouds which are coincident with regions of enhanced flux

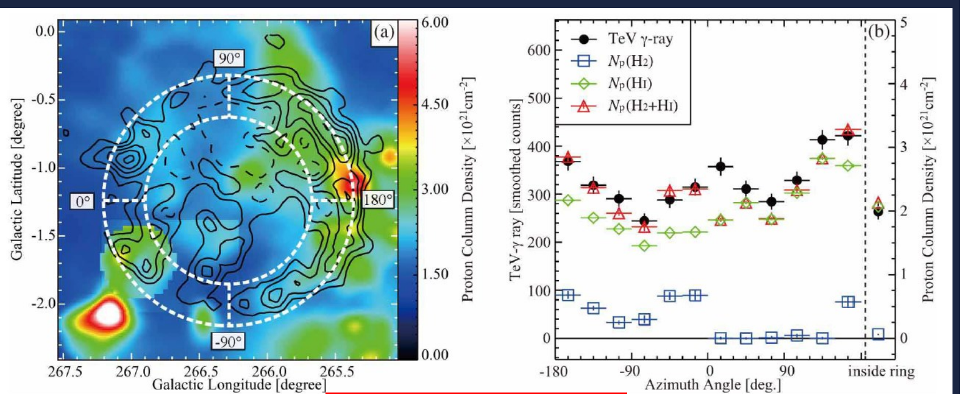

see Fukui's talk

Fukui 2013

Pulsar wind nebula

- PSR J0852.0-4622
  - Characteristic age of 140 kyr
  - Spin-down luminosity $1.1 \cdot 10^{36}$ erg
  - Closer than 900 pc
  - X-ray PWN detected
- We don't know the size of the potential TeV PWN, so several regions are assumed and emission from these regions is considered as an upper limit
- Region B: a hint of deviation of the spectrum w.r.t. the rest of SNR – constrains the size?
- Upper limit on the gamma-ray efficiency (above 1 TeV) is 10^{-4} – compatible with other PWNe
- Contamination of the SNR emission by PWN emission can be up to 8%

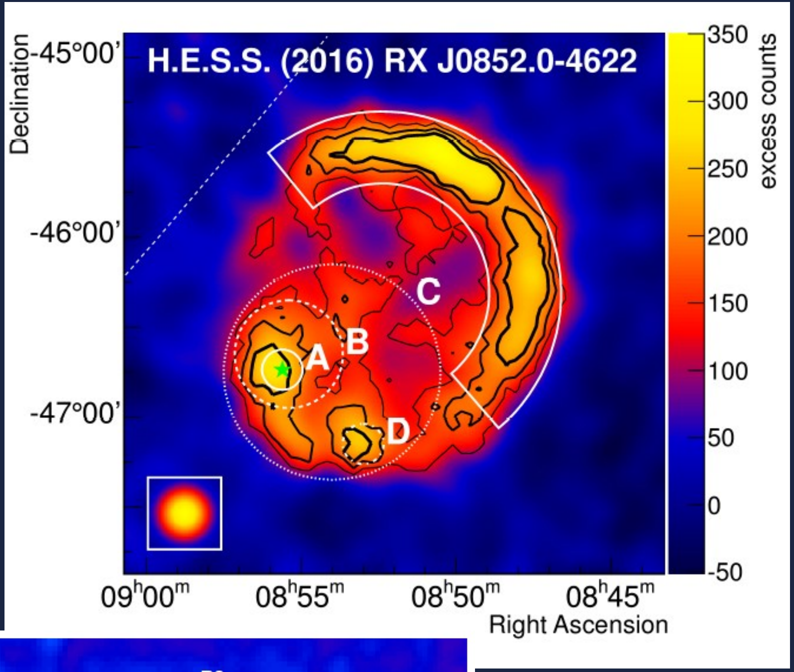

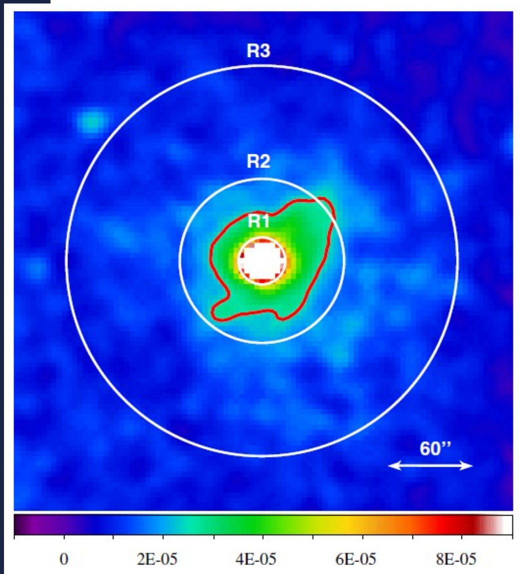

Acero et al 2013

Summary

- A revised flux measurement makes Vela Jr. the brightest steady source above 1 TeV
- The energy spectrum exhibits a clear curvature with an exponential cut-off at $E_{cut} = 6.7 \pm 1.2_{stat} \pm 1.2_{syst}$ TeV
- The new TeV spectrum connects well to Fermi measurement at GeV energies enabling direct determination of the characteristics of the present-time parent particle population in both leptonic and hadronic scenario
- Spatially-resolved spectroscopy study shows no clear spectral variation
- The enhancement of the flux detected towards PSR J0855-4644 suggests a possible contamination by the TeV PWN up to 8% of the total flux from the remnant

Back-up slides

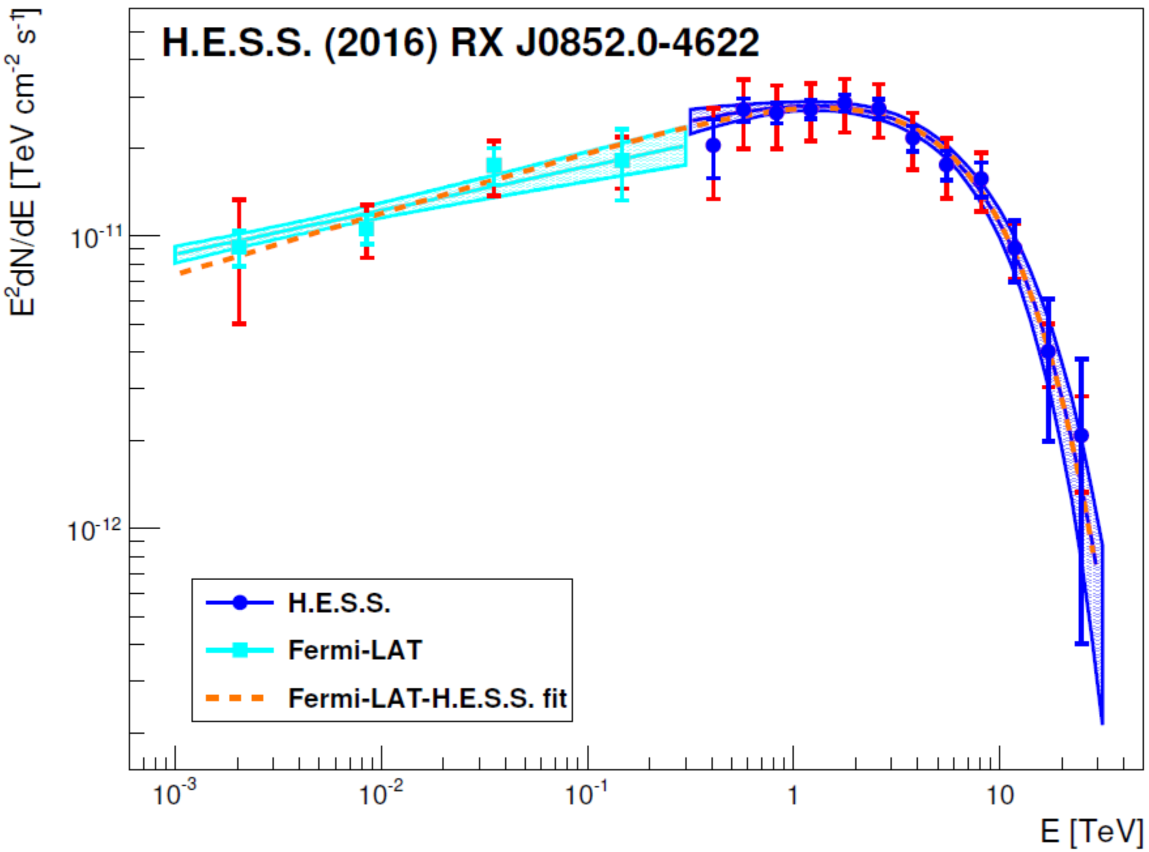

model	Φ_0 [cm^{-2}s^{-1}TeV^{-1}]	Γ	β	$E_{\rm cut}$ [TeV]	$\log L$	NFP	significance
PL	$(27.4 \pm 0.9)\ 10^{-12}$	2.30 ± 0.03	n/a	n/a	-51.717	2	n/a
CPL	$(28.8 \pm 1.1)\ 10^{-12}$	1.89 ± 0.07	0.23 ± 0.04	n/a	-24.567	3	7.3σ
ECPL	$(32.2 \pm 1.5)\ 10^{-12}$	1.81 ± 0.08	n/a	6.7 ± 1.2	-21.623	3	7.7σ

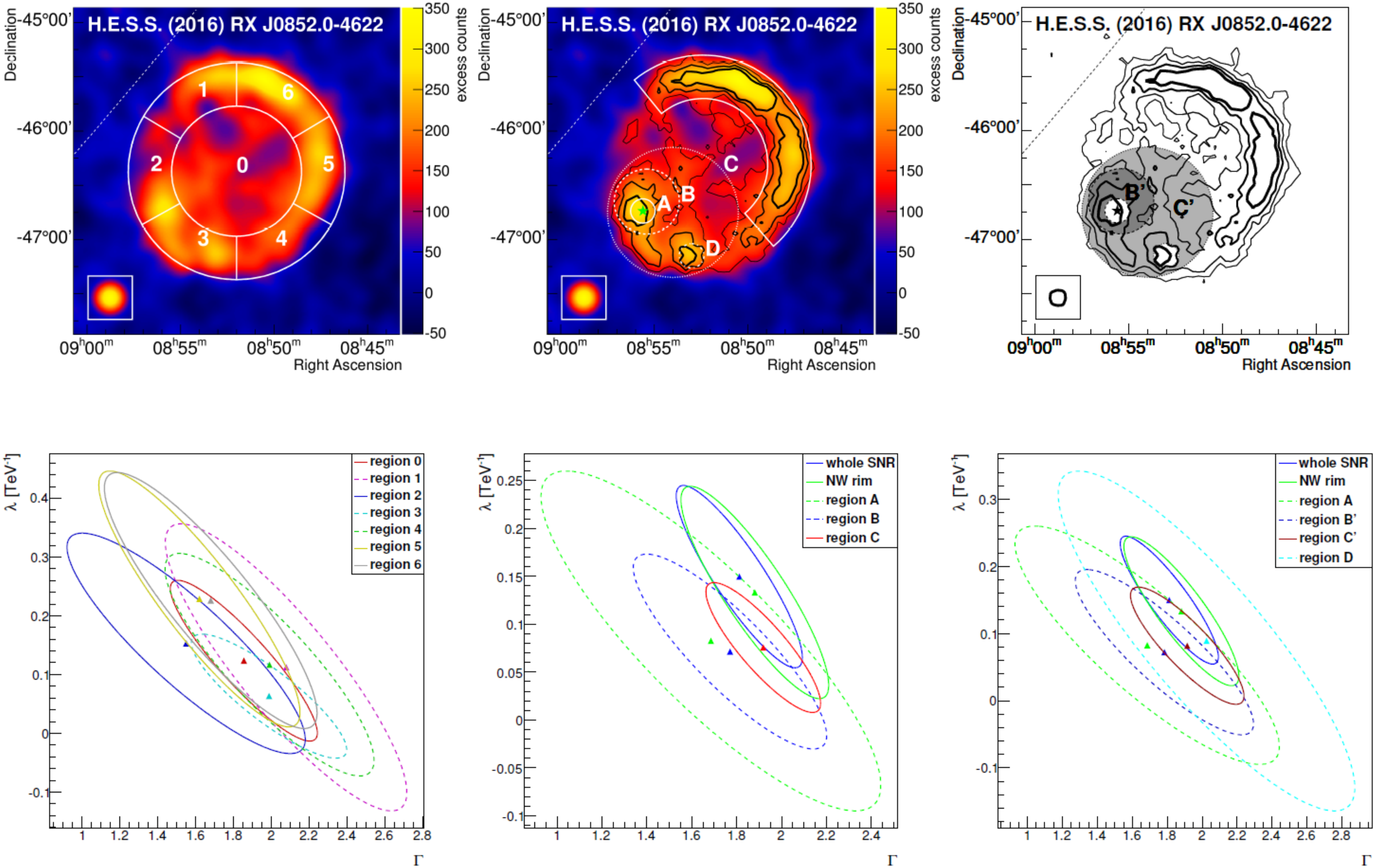
H.E.S.S. (2016) RX J0852.0-4622
Declination
Right Ascension
excess counts
-45°00'
-46°00'
-47°00'
09h00m
08h55m
08h50m
08h45m
0
1
2
3
4
5
6
A
B
C
D
B'
C'
350
300
250
200
150
100
50
0
-50
λ [TeV⁻¹]
Γ
region 0
region 1
region 2
region 3
region 4
region 5
region 6
whole SNR
NW rim
region A
region B
region C
region B'
region C'
region D